Accepted Manuscript

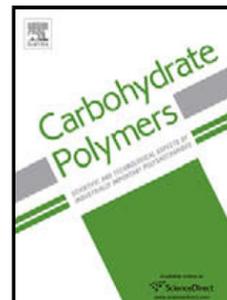1 **Supramolecular structure of jackfruit seed starch and its relationship with digestibility and**

2 **physicochemical properties**

3

4 Jin Chen [a], Yi Liang [b], Xiaoxi Li [a], Ling Chen [a,*] and Fengwei Xie [c,†]

5

6 [a] *Ministry of Education Engineering Research Center of Starch & Protein Processing, Guangdong Province*

7 *Key Laboratory for Green Processing of Natural Products and Product Safety, School of Food Science and*

8 *Engineering, South China University of Technology, Guangzhou, Guangdong 510640, China*

9 [b] *Guangdong Zhongqing Font Biochemical Science and Technology Co. Ltd., Maoming, Guangdong 525427,*

10 *China*

11 [c] *School of Chemical Engineering, The University of Queensland, Brisbane, Qld 4072, Australia*

12

[*] Corresponding author. Tel.: +86 20 8711 3252; fax: +86 20 8711 3252. *Email address:* felchen@scut.edu.cn (L. Chen)

[†] Corresponding author. Tel.: +61 7 3346 3199; fax: +61 7 3346 3973. *Email addresses:* f.xie@uq.edu.au, fwhsieh@gmail.com (F. Xie).

ABSTRACT

The influence of supramolecular structure on the physicochemical properties and digestibility of jackfruit seed starch (JSS) were investigated. Compared with maize and cassava starches (MS and CS), JSS had smaller granules and higher amylose content (JSS: 24.90%; CS: 16.68%; and MS: 22.42%), which contributed to higher gelatinization temperature (T_o: 81.11°C) and setback viscosity (548.9 mPa·s). From scanning electron microscopy, the digestion of JSS was observed mainly at the granule surface. Due to its higher crystallinity (JSS: 30.6%; CS: 30.3%; and MS: 27.4%) and more ordered semi-crystalline lamellae, JSS had a high RS content (74.26%) and melting enthalpy (19.61 J/g). In other words, the supramolecular structure of JSS extensively determined its digestibility and resistance to heat and mechanical shear treatment.

35

36

37

38 **Highlights:**

39 ✓ Jackfruit seed starch (JSS) had higher resistant starch content than other starches

40 ✓ High crystallinity and ordered semi-crystalline lamellae were the major reasons for the

41 higher enzyme-resistance of JSS

42 ✓ Digestion of JSS occurred mainly at the granule surface

43 ✓ Digestion caused slight decrease in crystallinity and lamellar regularity of JSS

44

45

46

47

48

49

50

51

52

53

54

55

56

57

58 Chemical compounds studied in this article

59 Starch (PubChem CID: 24836924); Sodium hydroxide (PubChem CID: 14798); Water (PubChem

60 CID: 962); Hydrochloric acid (PubChem CID: 313); Ethanol (PubChem CID: 702); Acetic acid

61 (PubChem CID: 176); Iodine (PubChem CID: 807); Potassium iodine (PubChem CID: 4875);

62 Sodium acetate (PubChem CID: 517045).

63

64

65 **1. Introduction**

66   Starch is one of the most important carbohydrates in human diets and has been extensively used

67 as a food ingredient. Understanding starch digestibility is of great interest to food industry and

68 importance for diet-related disorders such as obesity, diabetes, and cardiovascular diseases. Not all

69 starch can be digested in the small intestine, where the portion of starch that is not digested is

70 termed resistant starch (RS) (Asp & Björck, 1992). Physiological benefits have been correlated to

71 the RS consumption (Englyst & Hudson, 1996; Jenkins et al., 1998), which notably alters fecal bulk

72 and short-chain fatty acid metabolism, thus promoting the colonic health (Jenkins et al., 1998).

73   Because hydrolysis influences all level of food processing and nutrition, several arguments

74 prevail for a closer examination of the effects of hydrolytic enzymes on native starch granules. The

75 hydrolysis process of starches includes the diffusion of enzymes to the granule surface, followed by

76 the adsorption and subsequent catalytic events (Colonna, Leloup & Buleon, 1992). Previous studies

77 have shown that the action of α-amylase on starches from different botanical origins results in

78 varied digestion kinetics and degradation patterns (Fuwa, Takaya, Sugimoto & Marshall, 1980;

79 Sarikaya, Higasa, Adachi & Mikami, 2000). Generally, starch is a mixture of two types of

80 macromolecules, amylose and amylopectin (Hizukuri, 1985). Double or single helices of amylose

81 and amylopectin can be packed to form amorphous and crystalline regions (Oates, 1997), which is

82 the basis of the supramolecular structure (granule morphology, fractal structure, lamellar structure,

83 and crystalline structure) of starch. There are many structural factors of starch that affect the pattern

84 and rate of enzymatic hydrolysis, such as the size and shape of granules, granule integrity, porosity

85 of granules, crystallinity, amylose/amylopectin ratio, phosphate content, proteins, and lipids on the

86 granule surface (Copeland, Blazek, Salman & Tang, 2009; Dona, Pages, Gilbert & Kuchel, 2010;

87 Planchot, Colonna, Gallant & Bouchet, 1995; Robertson, Wong, Lee, Wagschal, Smith & Orts,

88 2006; Tester, Qi & Karkalas, 2006). The features of native starch granules that control the site, rate

89 and extent of hydrolysis by α-amylase are interrelated and not easily definable. Thus, studying the

90 changes of supramolecular structure would help to build the ability to manipulate and understand

91 the hydrolysis of starch granules.

92   Jackfruit is one of the most popular tropical fruits grown in Asia especially in Thailand. Its

93 seeds take up 10–15% of the whole fruits and contain abundant starch and proteins. With the rapid

94 development of the cultivating and processing industry of jackfruit, however, most seeds are

95 discarded, which causes a huge waste of starch resource. Jackfruit seed starch has not been

96 considered and exploited as a potent source of starch. To solve this problem, there have been studies

97 on the isolation and the properties of starch extracted from jackfruit seeds to verify its applicability

98 in food, pharmaceutics and other uses. Jackfruit seed starch has the Type-A crystallinity pattern and

99 a high amylose content (Madruga, de Albuquerque, Silva, do Amaral, Magnani & Neto, 2014).

100 Compared with other starches, jackfruit seed starch has significantly higher gelatinization

101 temperature and lower breakdown viscosity, suggesting that this starch can be used to products

102 where a high level of gelatinization is not desirable during cooking (Bobbio, EI-Dash, Bobbio &

103 Rodrigues, 1978; Kittipongpatana & Kittipongpatana, 2011; Rengsutthi & Charoenrein, 2011;

104 Theivasanthi & Alagar, 2011; Tulyathan, Tananuwong, Songjinda & Jaiboon, 2002; Yi &

105 Shenghong, 2006). However, the literature provides little information about the structural features

106 of jackfruit seed starch and its effects on different properties. In particular, while the supramolecular

107 structure and its effect on the hydrolysis of native jackfruit seed starch are essential to ensure the

108 nutritional value and a diverse range of food industry uses, this information has not been reported so

109 far.

110   The aim of the present study was to investigate the functional properties and enzyme digestion

111 of jackfruit seed starch, as well as the related hierarchical structure changes in the native starch

112 granule that control the susceptibility of starch to enzymatic hydrolysis. The results of jackfruit seed

113 starch were compared with cassava starch and maize starch, which are two of the most popular

114 starches used in food industry. This would provide us with nutritional implications which are

115 instrumental for practical applications.

116

117 **2.   Materials and methods**

118 *2.1.   Materials*

119   Jackfruit Seed Starch (JSS) was isolated from jackfruit seeds using a modified method of

120 (Bobbio, EI-Dash, Bobbio & Rodrigues, 1978). The seeds were manually separated from the

121 mucilage, and then the aril and spermoderm were peeled off. The peeled seeds were slurried in a

122 Waring Blender (HR 1727 Philips, Zhuhai, China) with an equal weight of a 0.1% sodium

123   hydroxide solution for approximately 10 min. Then, the slurry was pressed through multiple gauzes

124   to remove seed fibers. The resulting milking suspension was allowed to decant at 4−5°C and

125   rewashed with distilled water to eliminate soluble sugars. The supernatant was drained, and the

126   upper brown sediment was scraped. The remaining sediment was mixed with 0.1% sodium

127   hydroxide solution and filtered through a sieve (0.058 mm mesh size) to eliminate fibers. When the

128   supernatant became clear, the filtrate was neutralized with 0.1M hydrochloric acid to pH 7.0, and

129   the slurry was centrifuged at 3,000 g for 20 min. The starch was dried at 40°C for 24 h. The starch

130   was grounded with a mortar, passed through a sieve (0.15 mm mesh size), packed in a plastic bag

131   and kept at room temperature until further use. The yield of JSS from Jackfruit seed was

132   25.45–27.34 g/100 g (dry basis).

133   Cassava starch (CS) was purchased from Vietnamese Food and Investment Co., Ltd. (Nanning,

134   China). Maize starch (MS) was from Inner Mongolia Wang Yu Biotechnology Co., Ltd. (Inner

135   Mongolia, China). The moisture contents of JSS, CS, and MS, determined using a moisture

136   analyzer (DHS20-1, Sartorius Stedim Biotech GmbH, Germany), were 13.03%, 13.44%, and

137   13.25%, respectively. Porcine pancreatic α-amylase and amyloglucosidase were purchased from

138   Sigma-Aldrich (St. Louis, MO, USA). A glucose-oxidase peroxidase (GOPOD) assay kit was from

139   Megazyme International Ireland, Ltd. (Wicklow, Ireland). Potato amylose was purchased from

140   Heilongjiang Academy of Agricultural Sciences (Harbin, China).

141

142   *2.2.   Starch characterization*

143   *2.2.1.   Amylose content analysis*

144   The RS content of each sample (JSS, CS, and MS) was determined using a modified method of

145   ISO 6647-2:2007, of the International Standardization Organization (ISO, 2007).

146   0.1 g of the starch (dry basis) was accurately weighed and dissolved in 1 ml of ethanol and 9 ml

147   of sodium hydroxide solution (1 M), then heated in boiling water for 10 min. After cooling off, this

148   solution was then diluted to 100 mL in a volumetric flask with deionized water. An aliquot (2.50

149   mL) of this solution was then diluted with 25.00 mL of water, 0.50 mL of acetic acid solution (1 M),

150   0.50 mL of I_2/KI solution (0.0025 M I_2, and 0.0065 M KI), and the absorbance of this solution was

151   read in a 1cm path length quartz cell at 620 nm using an Evolution UV/Visible spectrophotometer

152   (Thermo Scientific, Waltham, USA). The amylose from potato (amylose content: 97.0%) was used

153   for the calibration curve (R^2=0.9962).

154

155   *2.2.2. Differential scanning calorimetry (DSC)*

156   Thermal behaviors of JSS, CS, and MS were studied using a PerkinElmer DSC 8000

157   (PerkinElmer, Waltham, America) with an internal coolant (Intercooler 2P) and nitrogen purge gas.

158   A high-pressure stainless steel pan (PerkinElmer No. B0182901) with a gold-plated copper seal

159   (PerkinElmer No. 042-191758) was used to achieve a constant moisture content (MC) during DSC

160   measurements. The sample, with about 70% MC, was prepared by premixing the starch with added

161   water in a sealed glass vial, which was kept at 20°C for 24 h before measurement. About a 4 mg

162   (dry basis) sample, scanned from 40 to 120°C, was used in this study. A slow heating rate of

163   5°C/min was used. The onset temperature (T_o), peak temperature (T_p), conclusion temperature (T_c),

164   and enthalpy (ΔH) of starch gelatinization were calculated. The enthalpy was calculated based on

165   the weight of dry basis starch.

166

167   *2.2.3. Pasting properties*

168   Pasting properties were studied using an Anton Paar MCR302 (Anton Paar China, Shanghai,

169   China). The sample slurry (6% concentration, starch on dry basis), after 1 min pre-shearing, was

170   heated from 30°C to 95°C at a heating rate of 5°C/min, held at 95°C for 15 min, and cooled to 50°C

171   at 5°C/min. Then the sample was held at 50°C for 15 min. The changes of viscosity were recorded.

172

173   *2.3. Enzyme digestion of starches*

174   *2.3.1. In vitro digestibility of native starches*

175   For native JSS, CS, and MS, the starch digestibility was determined following the modified

176   method of Englyst (Englyst, Kingman & Cummings, 1992). Based on the rate of hydrolysis, starch

177   was defined as rapidly-digestible starch (RDS, digested within 20 min), slowly-digestible starch

178   (SDS, digested between 20 min and 120 min), and resistant starch (RS, undigested within 120 min).

179   In brief, porcine pancreatic α-amylase (3 g) was dispersed in water (20 mL), stirred for 10 min

180   and centrifuged at 3000 g for 15 min. The supernatant (13.5 mL) was transferred to a beaker, and

181   225 U of amyloglucosidase and 1 mL of deionized water were added to the solution. The enzymatic

182   solution should be freshly prepared for each digestion. Duplicate samples (one named Sample A,

183   the other Sample B) of each starch (JSS, CS, and MS) (1 g, dry basis) were dispersed in 20 mL of

184   0.1 M sodium acetate buffer (pH = 5.2) and then mixed with an enzyme solution (5 mL) consisting

185   of the pancreatic extract and amyloglucosidase. The dispersion was incubated in a 37 °C shaking

186   water-bath at 180 strokes/min. An aliquot (0.5 mL) of Sample A was taken at interval of 20 min and

187   mixed with 20 ml of 70% ethanol. The mixed solution of Sample A was centrifuged at 3000 g for 10

188   min, and then the supernatant was used for hydrolyzing the glucose content, measured by the

189 glucose oxidase-peroxidase reagent. Sample B was mixed with ethanol to eliminate the activities of

190 enzyme, and then the dispersion was centrifuged at 3,000 g for 20 min. After three times of mixing

191 with ethanol and centrifugation, the sediments of Sample B were dried at 40°C for 12 h, named

192 JSS-20, CS-20, and MS-20 ("20" means the time interval (min) for which the three starches were

193 hydrolyzed), respectively. When the time interval reached 120 min, another aliquot (0.5 mL) of

194 Sample A was taken and mixed with 20 ml of 70% ethanol, centrifuged to analyze the hydrolyzed

195 glucose content. The sediments were treated using the same method of Sample B. These sediments

196 were JSS-120, CS-120, and MS-120, respectively.

197 *2.3.2. Scanning electron microscopy (SEM)*

198 　　Granule morphology was studied using an EVO18 scanning electron microscope (ZEISS,

199 Germany) operated at a high voltage of 10.0 kV. Before the SEM examination, the samples were

200 coated with a gold thin film.

201

202 *2.3.3. Small-angle X-ray scattering (SAXS)*

203 　　A SAXSess small angle X-ray scattering system (Anton Paar, Austria), operated at 50 mA and

204 40 kV, using Cu Kα radiation with a wavelength of 0.1542 nm as the X-ray source, was applied to

205 perform the SAXS measurements according to our previously method (Zhu, Li, Chen & Li, 2012)

206 with proper modification. Each sample was placed in a paste sample cell and exposed at the

207 incident X-ray monochromatic beam for 10 min. The data, recorded using an image plate, were

208 collected by the IP Reader software with a PerkinElmer storage phosphor system.

209 　　The samples used for the SAXS measurement were prepared by premixing the starch with

210 added water in glass vials and were equilibrated at 20°C for 24 h before the analysis. The total MC

211   of each sample was 65%. All data were normalized, and the background intensity and smeared

212   intensity were removed using the SAXSquant 3.0 software for further analysis.

213

214   *2.3.4. Polarized light microscopy*

215   Polarized light microscopy was performed using a polarized light microscope (PLM)

216   (Axioskop 40 Pol/40A Pol, ZEISS, Oberkochen, Germany) equipped with a 35mm SLA camera

217   (Power Shot G5, Canon, Tokyo, Japan). The magnification was 500 (50×10). Each sample was

218   dispersed as 10 mg (wet basis) of starch in 1 mL of distilled water in a glass vial. Then, a drop of

219   the starch suspension was transferred onto a slide and covered by a coverslip. Polarized light was

220   used for observation.

221

222   *2.3.5. X-ray diffraction (XRD)*

223   XRD analysis was performed with an Xpert PRO diffractometer (Panlytical, Netherlands),

224   operated at 40 mA and 40 kV, using Cu Kα radiation with a wavelength of 0.1542 nm as the X-ray

225   source. The scanning of diffraction angle (2θ) was from 5° to 40° with a scanning speed of 10°/min

226   and scanning step of 0.033°. The MC of each sample was about 10%. The relative crystallinity of

227   each sample was calculated using a previous method (Hermans & Weidinger, 1948).

228

229   *2.4 Statistical analysis*

230   The mean values and differences were analyzed using Duncan's multiple-range test. Analysis of

231   variance (ANOVA), followed by the least significant difference test (LSD-test), was performed

232   using the software SPSS (Version 22.0). The significance level was set at $p < 0.05$.

233

3.   Results and discussion

3.1.   Amylose contents and in vitro enzyme digestion analysis of native starches

The amylose/amylopectin ratio is an important index of starch and it can influence digestion

and swelling properties through the way of amylose and amylopectin packed. As seen from Table 1,

compared to CS and MS, the amylose content of JSS was higher (24.90%), which was similar to a

previous finding (Li & Zhong, 2004). CS had the lowest amylose content, only 16.68%. Based on

the Englyst test, the percentages of RDS, SDS, and RS in JSS were 5.92%, 19.82%, and 74.26%,

respectively. The RS content of JSS was much higher than CS and MS while RDS and SDS were

lower, indicating that JSS had strong anti-enzymatic capability. Interestingly, MS had the lowest RS

content but the highest SDS content, suggesting that it is a good material of SDS. The

slow-digestion property of MS is more likely to be controlled by its inherent structure (perhaps

amylopectin chain length distribution) although the existence of surface porous channels might

contribute to a high rate of starch hydrolysis (Zhang, Ao & Hamaker, 2006).

247

248

249

3.2.   Supramolecular structure characteristics of native and hydrolyzed starches

3.2.1.   Granule morphology

Fig. 1 shows the SEM images of JSS, CS and MS in their native states and after 20min and

120min enzyme hydrolysis. The JSS and CS granules had round to bell shapes with a smooth

surface. Unlike the other two starches, the MS granules were irregular in shape with small pores and

255   pits randomly distributed on a rough surface. The JSS granules were less irregular in shape, being

256   smaller than the CS and MS granules.

257

258

259

260   The susceptibility of starch granules can be classified by the degree and manner by which the

261   granules are eroded and corroded. As seen from SEM, the degree of digestion of starch followed the

262   order: MS > CS > JSS, contrary to the trend of RS (Table 1), which is as expected. Besides, the

263   observed levels of digestion were comparable between large and small granules for all three raw

264   starches. Some small granules in JSS-20 and CS-20 even became hollow with only a thin external

265   shell structure. This suggests a fundamental difference in the mode of α-amylase and

266   amyloglucosidase action, according to the granule size. Smaller granules, by virtue of their higher

267   available surface area per unit mass, facilitate the diffusion and adsorption of enzymes (Colonna,

268   Leloup & Buleon, 1992).

269   Digestion of JSS was not clearly apparent; the main indication was a less smooth and more

270   rugged granule surface with a few pits (JSS-20 and JSS-20, in Fig.1). Enzymatic digestion of CS

271   was apparent from the increased surface roughness and formation of deep cracks and large holes in

272   many granules (CS-20 and CS-120 in Fig.1). After 20min of enzymatic digestion, some CS granules

273   were in a truncated form (CS-20 in Fig.1). Truncatures are weak points in the granule structure that

274   lead to increased susceptibility, resulting in enhanced hydrolysis of CS. (Valetudie, Colonna,

275   Bouchet & Gallant, 1993). Because of no pores and smooth surfaces, SEM micrographs for JSS and

276   CS showed that enzymatic erosion occurred mainly at the surface. The MS granules showed

277   extensive corrosion, mainly in the direction of the radial axis and only a few granules remained

278   intact. The surface pores of hydrolyzed MS became larger and deeper into granules because of the

279   more extensive hydrolysis (MS-20 in Fig.1). After 120min hydrolysis, some granules were split,

280   exposing their layered internal structure (MS-120 in Fig.1). The layered internal structure showed

281   different susceptibility of the semi-crystalline structure and amorphous growth rings toward

282   digestion (Zhang, Ao & Hamaker, 2006).

283

284   *3.2.2. Lamellar structure characteristics*

285   The double-logarithmic SAXS patterns of native and hydrolyzed starch residues are shown in

286   Fig. 2. From this figure, we can obtain some parameters of a theoretical model for the lamellar

287   structure in starch (Cameron & Donald, 1993a, b), including d, the average thickness of the

288   semi-crystalline lamellae; $\Delta\rho = \rho_c - \rho_a$ (where ρ_c and ρ_a are the electron densies of the crystalline

289   regions and the amorphous regions in the semi-crystalline lamellae), the difference in electron

290   density between the crystalline lamellae and the amorphous lamellae; $\Delta\rho_u = \rho_u - \rho_a$ (where ρ_u is the

291   electron density of the amorphous background), the difference in election density between the value

292   of q of the peak at *ca.* 0.6 nm^{-1} can be used to calculate the average repeat distance (d) of the

293   semi-crystalline lamellae in starch granules according to the Woolf-Bragg's equation $d = 2\pi/q$

294   (Blazek & Gilbert, 2010; Vermeylen, Goderis & Delcour, 2006). Table 2 shows the SAXS

295   parameters from the peaks of native and hydrolyzed starches. It can be seen from Table 2 that the

296   average thickness of the semi-crystalline lamellae of JSS and CS were thinner than that of MS (JSS:

297   9.06 nm; CS: 9.14 nm; and MS: 9.42 nm) and the peak areas of JSS and CS were larger than MS

298   (JSS: 0.1288; CS: 0.1248; and MS: 0.0800). This indicates JSS and CS may have more ordered

299   semi-crystalline lamellae than MS.

300

301

302

303   The log $I \sim$ log q SAXS patterns of JSS, CS, and MS and their hydrolyzed residues are

304   presented in Fig. 2a, b and c. The scattering intensity changed slightly for JSS (JSS-20 and JSS-120

305   in Fig. 2a) during the whole enzymatic hydrolysis. After 120min hydrolysis, the scattering intensity

306   at the low q region showed an increasing trend (JSS-120 in Fig. 2a) and the definition of the peak of

307   JSS-120 was lower than those of JSS and JSS-20. This can be explained by the easier disturbance of

308   starch molecular arrangement in the amorphous background than in the amorphous lamellae by

309   α-amylase, thus resulting in an increase in $\Delta\rho_u$ (Cameron & Donald, 1992). All the analysis of JSS

310   showed that most of the semi-crystalline lamellae of JSS remained intact even after 120min

311   hydrolysis. And the slight changes in the scattering intensity of JSS, JSS-20, and JSS-120 explained

312   a high RS content of JSS and less obvious surface erosion. However for CS and MS (CS-20 in Fig.

313   2b and MS-20 in Fig. 2c), the q region around the peak showed a decreasing trend, suggesting the

314   crystalline regions in the semi-crystalline lamellae were disturbed after 20min hydrolysis. And the

315   scattering intensity at the low q region showed an increasing trend, due to more destruction to the

316   amorphous background than to the amorphous lamellae. After 120min hydrolysis (CS-120 in Fig.

317   2b and MS-120 in Fig. 2c), the scattering intensity decreased to an extensive degree. It is noted that

318   the decrease of scattering intensity in MS was faster during the first 20 min of enzymatic hydrolysis

319   and slower from 20 min to 120 min than in CS. This could be an excellent explanation for the

320   higher SDS content of MS. Based on the above discussion, a conclusion can be made that the

321   semi-crystalline lamellae of JSS were more ordered and thus more resistant to the hydrolysis than

322   those of CS and MS.

323

324   *3.2.3 Crystalline characteristics*

325   Normally, a birefringence cross can be observed when the starch granule is exposed under

326   polarized light, due to orderly-arranged starch molecules of crystalline regions and

327   disorderly-arranged starch molecules of amorphous regions. Therefore, information about the

328   crystalline structure of starch can be reflected by the birefringence pattern when starch granules

329   suffered from hydrolysis or external attack. The polarized light microscope images of JSS, CS, and

330   MS and their hydrolyzed residues are shown in Fig. 3. Given the different sizes of JSS, CS, and MS

331   granules, native JSS showed weaker birefringence intensity than CS and MS, while CS showed the

332   strongest intensity. It is noted that the birefringence intensity remained almost the same for JSS after

333   enzyme hydrolysis for 120 min, suggesting most of crystalline structure of JSS was retained.

334   Nevertheless, the birefringence intensity decreased significantly for CS and MS (especially for MS),

335   and the birefringence crosses became less apparent, owing to the disturbance of double helices in

336   their crystallites during enzyme digestion. This result is consistent with the analysis of SAXS.

337

338

339

340   Fig. 4 shows the XRD patterns of JSS, CS, and MS, and their hydrolyzed residues. It is seen

341   that JSS and MS displayed a typical A-type crystalline structure with main diffraction peaks at *ca.*

342   15, 17, 18 and 23° (2θ) (Tulyathan, Pananuwong, Songjinda & Jaiboon, 2002; Zobel, 1964). CS

343   exhibited a weak diffraction maximum at 5.6°(2θ), and the 17°(2θ) peak was somewhat more

344   intense than its 18° (2θ) neighbor (Chrastil, 1987). Both features indicated CS contained some

345   B-type crystalline structure but the main structure was still A-type. The degree of relative

346   crystallinity of starch followed the order: JSS ≈ CS > MS. According to the XRD patterns of

347   partly-digested starches of JSS, CS and MS, the crystalline types of all three starches remained

348   essentially unchanged after digestion. However, after enzyme treatment, decreased diffraction

349   intensities were observed (Figure 4a, b, and c). The relative crystallinity of JSS changed moderately,

350   decreased from 30.6% to 27.6% (Table 2) after 20min digestion, while CS and MS decreased more

351   sharply from 30.3% to 23.6% and 27.4% to 19.4%, respectively. These results suggest that

352   hydrolysis did occur in the crystalline regions despite that most of crystalline structure of JSS was

353   retained after 120min hydrolysis.

354

355   It is noted that although JSS and CS both had a smooth surface and similar relative crystallinity

356   (Table 2), the RS content of JSS was higher than CS. This can be demonstrated by the observation

357   that the degree of the ordered structure in semi-crystalline lamellae was in the order JSS﹥CS﹥MS

358   in the SAXS, suggesting not only the crystallinity but the way how molecules are ordered play a

359   key role in the enzyme digestion of JSS. Another reason could be due to their amylose/amylopectin

360   ratio. Specifically, a higher amylose content may mean an increased number of long chains and

361   facilitate the amylose-lipid complex formation on the granule surface, leading to an increased

362   content of enzyme-resistant starch (Crowe, Seligman & Copeland, 2000; Cui & Oates, 1999;

363   Tufvesson, Skrabanja, Björck, Elmståhl & Eliasson, 2001). The surface pores and low relative

364   crystallinity of MS could contribute to its high RDS and low RS contents.

365   When the α-amylase attacks starch granules, the double helices must first be unwound, as

366   single-stranded helices are the polymeric substrates for the enzyme (Larson, Day & McPherson,

367   2010). The amylopectin double helices can only be unwound if they are dissociated from their

368   crystallites. However, the amylopectin side chains of starch strongly interact, not only with their

369   helical duplex partners, but also with other neighboring helices. Thus, more ordered crystalline

370   structure leads to a lower rate of enzymatic hydrolysis because of stronger interactions between

371   neighboring helices. Normally, higher crystallinity is in consistent with more ordered arrangement

372   of amylopectin double helices in the semi-crystalline lamellae, since the crystallinity reflects the

373   long range order of starch. In the light of these principles, the more ordered crystalline structure

374   (corresponding to more ordered semi-crystalline lamellae and high relative crystallinity) was the

375   main reason for the strong anti-enzymatic capability of JSS.

376

377   *3.3.   Thermal behavior*

378   Fig.5a shows the DSC thermograms of JSS, CS and MS in excess water (70 wt.%) and the

379   related thermal parameters were shown in Table 3. From Fig.5a and Table 3, it was obvious that JSS

380   had the highest gelatinization temperature (T_o: 81.11°C), followed by MS (T_o: 65.58°C) and CS (T_o:

381   60.47°C). The higher T_o, T_p, and T_c of JSS could be due to a higher content of amylose-lipid

382   complexes with an increased amylose content, resulting in reduced swelling of the granule

383   (Karkalas & Raphaelides, 1986; Pycia, Juszczak, Gałkowska & Witczak, 2012; Svihus, Uhlen &

384   Harstad, 2005; Tester & Morrison, 1990). The higher gelatinization temperature of JSS may also

385   reflect its much longer amylopectin chains, as there is a significant positive correlation between the

386   DSC gelatinization parameters and the amylopectin unit-chain length distribution of starches (Jane

387   et al., 1999; Noda et al., 1998; Shi & Seib, 1995; Srichuwong, Sunarti, Mishima, Isono &

388   Hisamatsu, 2005a). Since the granule size followed the order CS‧MS‧JSS (Fig.1), another reason

389   could be related to the size of starch granules since larger granules might be more vulnerable during

390   heating (Chiotelli & Le Meste, 2002; Kaur, Singh & Sodhi, 2002; Vasanthan & Bhatty, 1996). JSS

391   and MS showed rather symmetric peaks and had similar ΔT, which was narrower than that of CS.

392   This indicates that the crystalline structure of JSS and MS are more unified and consistent than that

393   of CS, resulting in more homogeneous heat conductivity. Higher ΔT of CS was proposed to arise

394   from the inconsistency of crystalline structure corresponding to the melting of B-type in CS

395   although the main structure in CS was A-type. JSS and CS had similar ΔH (Table 3), due to their

396   similar relative crystallinity, which were higher than that of MS.The higher ΔH values suggested

397   that the interactions (via hydrogen bonding) between double helices (which were packed in clusters)

398   forming the crystalline regions of JSS and CS were probably more extensive than in MS (Cooke &

399   Gidley, 1992; Zhou, Hoover & Liu, 2004).

400

401

402

403

404   *3.4.   Pasting properties*

405   Fig.5b shows the pasting properties of JSS, CS and MS. As seen from Table 3, the peak

406   viscosity (PV) of three starches followed the order JSS‧CS‧MS, which corresponded to the trend

407   of T_o. The breakdown viscosity (BDV) of JSS (109.5 mPa·s) was lower than those of CS and MS

408   (473.2 mPa·s and 288.4 mPa·s, respectively). When viscosity reached PV, almost all of amylose

409   leached out and therefore BDV was less affected by amylose, but more by amylopectin fine

410   structure (Han & Hamaker, 2001). Lower BDV is another indicator that JSS may have much longer

411   amylopectin chains since dissociation of double helices of amylopectin leads to granule swelling

412   and affects pasting properties to some extent (Han & Hamaker, 2001; Srichuwong, Sunarti,

413   Mishima, Isono & Hisamatsu, 2005b). The final viscosity (FV) and setback viscosity (SBV)

414   indicate the re-association of the starch molecules involving amylose after gelatinization and a

415   formation of a gel network (Charles, Chang, Ko, Sriroth & Huang, 2004). JSS had higher FV and

416   SBV than CS and MS (Table 3), owing to a high amylose content (Sasaki, Yasui & Matsuki, 2000;

417   Vandeputte, Derycke, Geeroms & Delcour, 2003). The reason CS had less amylose content but

418   higher FV and SB than MS might be due to the finer amylopectin structure (enrichment in B2

419   chains) of CS (Srichuwong, Sunarti, Mishima, Isono & Hisamatsu, 2005b).

420

421   **4.   Conclusion**

422   JSS granules were shown to be small, round to bell shapes, with a smooth surface and

423   displayed a typical A-type crystalline structure. Compared with MS and CS, JSS had higher

424   amylose content, higher RS content and more ordered semi-crystalline lamellae. According to the

425   DSC measurement, JSS had the highest T_o. This might be because of the reduced swelling of the

426   granule, probably due to more amylose-lipid complexes with higher amylose content and to its

427   smaller granules which were more resistance to heat. JSS and CS had similar ΔH, due to their

428   similar relative crystallinity. From the pasting property study, the BDV of JSS was lower than those

429   of CS and MS while FV and SBV were higher. Lower BDV might indicate longer amylopectin

430 chains of JSS, which needs further investigation. As seen from SEM, the degree of digestion of

431 starch followed the order: MS > CS > JSS. Digestion of JSS only apparently occurred at the surface,

432 with a less smooth and more rugged granule surface with occasional pitting. In the course of

433 digestion, for JSS, the scattering intensity and the relative crystallinity were decreased slightly, and

434 the birefringence intensity remained almost the same. These observations indicate the more ordered

435 semi-crystalline lamellae and high relative crystallinity were the major factors for the stronger

436 anti-enzymatic capability of JSS than those of CS and MS. In conclusion, the results presented the

437 detailed related supramolecular structure changes (especially granular, crystalline, and lamellae

438 structure) of JSS granules that control the susceptibility of starch to enzymatic hydrolysis and the

439 physicochemical properties. The knowledge obtained from this work is expected to facilitate further

440 research on the nutritional and other properties of JSS for widening its industrial application.

441

452

453   **References**

454   Asp, N.-G., & Björck, I. (1992). Resistant starch. *Trends in Food Science & Technology, 3*,

455   111-114.

456

457   Blazek, J., & Gilbert, E.P. (2010). Effect of enzymatic hydrolysis on native starch granule

458   structure. *Biomacromolecules, 11*(12), 3275-3289.

459

460   Bobbio, F., EI-Dash, A., Bobbio, P., & Rodrigues, L. (1978). Isolation and characterization of

461   the physicochemical properties of the starch of jackfruit seeds (Artocarpus heterophyllus). *Cereal*

462   *Chemistry*.

463

464   Cameron, R.E., & Donald, A.M. (1992). A small-angle X-ray scattering study of the annealing

465   and gelatinization of starch*.

466

467   Cameron, R.E., & Donald, A.M. (1993a). A small-angle X-ray scattering study of the

468   absorption of water into the starch granule. *Carbohydrate Research, 244*(2), 225-236.

469

470   Cameron, R.E., & Donald, A.M. (1993b). A small‐angle x‐ray scattering study of starch

471   gelatinization in excess and limiting water. *Journal of Polymer Science Part B: Polymer Physics,*

472   *31*(9), 1197-1203.

473

474   Charles, A.L., Chang, Y.H., Ko, W.C., Sriroth, K., & Huang, T.C. (2004). Some physical and

475   chemical properties of starch isolates of cassava genotypes. *Starch ‑ Stärke, 56*(9), 413-418.

476

477   Chiotelli, E., & Le Meste, M. (2002). Effect of small and large wheat starch granules on

478   thermomechanical behavior of starch. *Cereal chemistry, 79*(2), 286-293.

479

480   Chrastil, J. (1987). Improved colorimetric determination of amylose in starches or flours.

481   *Carbohydrate Research, 159*(1), 154-158.

482

483   Colonna, P., Leloup, V., & Buleon, A. (1992). Limiting factors of starch hydrolysis. *European*

484   *journal of clinical nutrition, 46*, S17-32.

485

486   Cooke, D., & Gidley, M.J. (1992). Loss of crystalline and molecular order during starch

487   gelatinisation: origin of the enthalpic transition. *Carbohydrate Research, 227*, 103-112.

488

489   Copeland, L., Blazek, J., Salman, H., & Tang, M.C. (2009). Form and functionality of starch.

490   *Food Hydrocolloids, 23*(6), 1527-1534.

491

492   Crowe, T.C., Seligman, S.A., & Copeland, L. (2000). Inhibition of enzymic digestion of

493   amylose by free fatty acids in vitro contributes to resistant starch formation. *The Journal of*

494   *nutrition, 130*(8), 2006-2008.

495

496   Cui, R., & Oates, C. (1999). + The effect of amylose–lipid complex formation on enzyme

497   susceptibility of sago starch. *Food Chemistry, 65*(4), 417-425.

498

499   Dona, A.C., Pages, G., Gilbert, R.G., & Kuchel, P.W. (2010). Digestion of starch: In vivo and in

500   vitro kinetic models used to characterise oligosaccharide or glucose release. *Carbohydrate*

501   *Polymers, 80*(3), 599-617.

502

503   Englyst, H.N., & Hudson, G.J. (1996). The classification and measurement of dietary

504   carbohydrates. *Food Chemistry, 57*(1), 15-21.

505

506   Englyst, H.N., Kingman, S., & Cummings, J. (1992). Classification and measurement of

507   nutritionally important starch fractions. *European journal of clinical nutrition, 46*, S33-50.

508

509   Fuwa, H., Takaya, T., Sugimoto, Y., & Marshall, J. (1980). Mechanisms of Saccharide

510   Polymerisation and Depolymerisation'. Academic Press, New York.

511

512   Han, X.-Z., & Hamaker, B.R. (2001). Amylopectin fine structure and rice starch paste

513   breakdown. *Journal of Cereal Science, 34*(3), 279-284.

514

515   Hermans, P., & Weidinger, A. (1948). Quantitative X‐Ray Investigations on the Crystallinity

516   of Cellulose Fibers. A Background Analysis. *Journal of Applied Physics, 19*(5), 491-506.

517

518   Hizukuri, S. (1985). Relationship between the distribution of the chain length of amylopectin

519   and the crystalline structure of starch granules. *Carbohydrate Research, 141*(2), 295-306.

520

521   ISO. (2007). 6647-2:Rice—Determination of amylose content—Part 2.

522

523   Jane, J., Chen, Y., Lee, L., McPherson, A., Wong, K., Radosavljevic, M., & Kasemsuwan, T.

524   (1999). Effects of amylopectin branch chain length and amylose content on the gelatinization and

525   pasting properties of starch 1. *Cereal chemistry, 76*(5), 629-637.

526

527   Jenkins, D.J., Vuksan, V., Kendall, C.W., Würsch, P., Jeffcoat, R., Waring, S., Mehling, C.C.,

528   Vidgen, E., Augustin, L.S., & Wong, E. (1998). Physiological effects of resistant starches on fecal

529   bulk, short chain fatty acids, blood lipids and glycemic index. *Journal of the American College of*

530   *Nutrition, 17*(6), 609-616.

531

532   Karkalas, J., & Raphaelides, S. (1986). Quantitative aspects of amylose-lipid interactions.

533   *Carbohydrate Research, 157*, 215-234.

534

535   Kaur, L., Singh, N., & Sodhi, N.S. (2002). Some properties of potatoes and their starches II.

536   Morphological, thermal and rheological properties of starches. *Food Chemistry, 79*(2), 183-192.

537

538   Kittipongpatana, O.S., & Kittipongpatana, N. (2011). Preparation and physicochemical

539   properties of modified jackfruit starches. *LWT-Food Science and Technology, 44*(8), 1766-1773.

540

541   Larson, S.B., Day, J.S., & McPherson, A. (2010). X-ray crystallographic analyses of pig

542   pancreatic α-amylase with limit dextrin, oligosaccharide, and α-cyclodextrin. *Biochemistry, 49*(14),

543   3101-3115.

544

545   Li, X.-j., & Zhong, M. (2004). Study on Granular Morphology of Starch Isolated from

546   Jack-fruit Seeds. *Food Science, 6*, 012.

547

548   Madruga, M.S., de Albuquerque, F.S. M., Silva, I.R. A., do Amaral, D.S., Magnani, M., & Neto,

549   V.Q. (2014). Chemical, morphological and functional properties of Brazilian jackfruit (Artocarpus

550   heterophyllus L.) seeds starch. *Food chemistry, 143*, 440-445.

551

552   Noda, T., Takahata, Y., Sato, T., Suda, I., Morishita, T., Ishiguro, K., & Yamakawa, O. (1998).

553   Relationships between chain length distribution of amylopectin and gelatinization properties within

554   the same botanical origin for sweet potato and buckwheat. *Carbohydrate Polymers, 37*(2), 153-158.

555

556   Oates, C.G. (1997). Towards an understanding of starch granule structure and hydrolysis.

557   *Trends in Food Science & Technology, 8*(11), 375-382.

558

559   Planchot, V., Colonna, P., Gallant, D., & Bouchet, B. (1995). Extensive degradation of native

560   starch granules by alpha-amylase from Aspergillus fumigatus. *Journal of Cereal Science, 21*(2),

561   163-171.

562

563   Pycia, K., Juszczak, L., Gałkowska, D., & Witczak, M. (2012). Physicochemical properties of

564   starches obtained from Polish potato cultivars. *Starch ‐ Stärke, 64*(2), 105-114.

565

566   Rengsutthi, K., & Charoenrein, S. (2011). Physico-chemical properties of jackfruit seed starch

567   (Artocarpus heterophyllus) and its application as a thickener and stabilizer in chilli sauce.

568   *LWT-Food Science and Technology, 44*(5), 1309-1313.

569

570   Robertson, G.H., Wong, D.W., Lee, C.C., Wagschal, K., Smith, M.R., & Orts, W.J. (2006).

571   Native or raw starch digestion: a key step in energy efficient biorefining of grain. *Journal of*

572   *agricultural and food chemistry, 54*(2), 353-365.

573

574   Sarikaya, E., Higasa, T., Adachi, M., & Mikami, B. (2000). Comparison of degradation abilities

575   of α-and β-amylases on raw starch granules. *Process Biochemistry, 35*(7), 711-715.

576

577   Sasaki, T., Yasui, T., & Matsuki, J. (2000). Effect of amylose content on gelatinization,

578   retrogradation, and pasting properties of starches from waxy and nonwaxy wheat and their F1 seeds.

579   *Cereal chemistry, 77*(1), 58-63.

580

581   Shi, Y.-C., & Seib, P.A. (1995). Fine structure of maize starches from four wx-containing

582   genotypes of the W64A inbred line in relation to gelatinization and retrogradation. *Carbohydrate*

583   *Polymers, 26*(2), 141-147.

584

585   Srichuwong, S., Sunarti, T.C., Mishima, T., Isono, N., & Hisamatsu, M. (2005a). Starches from

586   different botanical sources I: Contribution of amylopectin fine structure to thermal properties and

587   enzyme digestibility. *Carbohydrate Polymers, 60*(4), 529-538.

588

589   Srichuwong, S., Sunarti, T.C., Mishima, T., Isono, N., & Hisamatsu, M. (2005b). Starches from

590   different botanical sources II: Contribution of starch structure to swelling and pasting properties.

591   *Carbohydrate Polymers, 62*(1), 25-34.

592

593   Svihus, B., Uhlen, A.K., & Harstad, O.M. (2005). Effect of starch granule structure, associated

594   components and processing on nutritive value of cereal starch: A review. *Animal Feed Science and*

595   *Technology, 122*(3-4), 303-320.

596

597   Tester, R., Qi, X., & Karkalas, J. (2006). Hydrolysis of native starches with amylases. *Animal*

598   *Feed Science and Technology, 130*(1), 39-54.

599

600   Tester, R.F., & Morrison, W.R. (1990). Swelling and gelatinization of cereal starches. I. Effects

601   of amylopectin, amylose, and lipids. *Cereal Chem, 67*(6), 551-557.

602

603   Theivasanthi, T., & Alagar, M. (2011). An insight analysis of nano sized powder of jackfruit

604   seed. *arXiv preprint arXiv:1110.0346*.

605

606   Tufvesson, F., Skrabanja, V., Björck, I., Elmståhl, H.L., & Eliasson, A.-C. (2001). Digestibility

607   of starch systems containing amylose–glycerol monopalmitin complexes. *LWT-Food Science and*

608   *Technology, 34*(3), 131-139.

609

610   Tulyathan, V., Tananuwong, K., Songjinda, P., & Jaiboon, N. (2002). Some physicochemical

611   properties of jackfruit (Artocarpus heterophyllus Lam) seed flour and starch. *Science Asia, 28*,

612   37-41.

613

614   Valetudie, J.C., Colonna, P., Bouchet, B., & Gallant, D.J. (1993). Hydrolysis of Tropical Tuber

615   Starches by Bacterial and Pancreatic α‐Amylases. *Starch‐Stärke, 45*(8), 270-276.

616

617   Vandeputte, G., Derycke, V., Geeroms, J., & Delcour, J. (2003). Rice starches. II. Structural

618   aspects provide insight into swelling and pasting properties. *Journal of Cereal Science, 38*(1),

619   53-59.

620

621   Vasanthan, T., & Bhatty, R. (1996). Physicochemical properties of small-and large-granule

622   starches of waxy, regular, and high-amylose barleys. *Cereal chemistry, 73*(2), 199-207.

623

624   Vermeylen, R., Goderis, B., & Delcour, J.A. (2006). An X-ray study of hydrothermally treated

625   potato starch. *Carbohydrate Polymers, 64*(2), 364-375.

626

627   Yi, L.X. H. C. H., & Shenghong, C.H. X. (2006). Starch Extraction and Its Characteristics of

628   Jack-fruit Seeds [J]. *Food and Fermentation Industries, 10*, 032.

629

630   Zhang, G., Ao, Z., & Hamaker, B.R. (2006). Slow Digestion Property of Native Cereal Starches.

631   *Biomacromolecules, 7*(11), 3252-3258.

632

633   Zhou, Y., Hoover, R., & Liu, Q. (2004). Relationship between α-amylase degradation and the

634   structure and physicochemical properties of legume starches. *Carbohydrate Polymers, 57*(3),

635   299-317.

636

637   Zhu, J., Li, L., Chen, L., & Li, X. (2012). Study on supramolecular structural changes of

638   ultrasonic treated potato starch granules. *Food Hydrocolloids, 29*(1), 116-122.

639

640   Zobel, H. (1964). X-ray analysis of starch granules. *Methods in carbohydrate chemistry, 4*,

641   109-113.

642

643

644

645

646   Figure Captions

647   Fig.1. SEM images of native and hydrolyzed starch residues at 1000× and 3000×magnification

648   Fig.2. Double-logarithmic SAXS patterns of native and hydrolyzed starch residues. (a) jackfruit

649   seed starch (JSS, JSS-20, and JSS-120); (b) cassava starch (CS, CS-20, and CS-120); (c) maize

650   starch (MS, MS-20, and MS-120).

651   Fig.3. Polarized light microscopic images of native and hydrolyzed starch residues

652   Fig.4. XRD patterns of native and hydrolyzed starch residues, (a) jackfruit seed starch (JSS,

653   JSS-20, and JSS-120); (b) cassava starch (CS, CS-20, and CS-120); (c) maize starch (MS, MS-20,

654   and MS-120).

655   Fig.5. Differential scanning calorimetry (DSC) thermograhs (a), and viscosity curves (b) of

656   jackfruit seed starch, cassava starch and maize starch

657

658   Tables

659   Table 1 Amylose contents and *in vitro* enzyme digestion analysis of jackfruit seed starch (JSS), cassava starch (CS) and

660   maize starch (MS).

Raw starches	RDS (%)	SDS (%)	RS (%)	Amylose (%)
Jackfruit seed starch (JSS)	5.92 ± 0.49^c	19.82 ± 1.01^c	74.26 ± 1.28^a	24.90 ± 0.10^a
Cassava starch (CS)	10.50 ± 0.04^b	38.43 ± 0.03^b	51.07 ± 0.08^b	16.68 ± 0.54^c
Maize starch (MS)	12.04 ± 0.04^a	69.73 ± 1.14^a	18.23 ± 1.18^c	22.42 ± 0.19^b

661   Values are means of three determinations (±standard deviation); values followed by the different letters within a column

662   differ significantly ($p < 0.05$).

663

664

665 Table 2. SAXS parameters and relative crystallinity of native and hydrolyzed starches.

Sample	q_{peak} (nm^{-1})	d (nm)	Peak Area	RC (%)
JSS	0.6934[abc]	9.06[de]	0.1288[a]	30.6[ab]
JSS-20	0.6868[bcd]	9.15[cd]	0.1240[a]	28.5[abcd]
JSS-120	0.7001[ab]	8.98[de]	0.0653[c]	27.6[bcd]
CS	0.6868[bcd]	9.14[de]	0.1248[a]	30.3[ab]
CS-20	0.6802[cd]	9.24[c]	0.0639[c]	25.4[def]
CS-120	0.6934[abc]	9.01[de]	0.0318[d]	23.6[efg]
MS	0.6670[e]	9.42[b]	0.0800[b]	27.4[cde]
MS-20	0.6604[e]	9.51[b]	0.0572[c]	21.5[g]
MS-120	0.6208[f]	10.12[a]	0.0213[d]	19.4[g]

666 Values are means of three determinations; values followed by the different letters within a column differ significantly (p

667 < 0.05).

668

669   Table 3 Gelatinization parameters and pasting properties of jackfruit seed starch (JSS), cassava starch (CS) and maize

670   starch (MS)

Sample	JSS	CS	MS
T_o (°C)	81.11±0.53[a]	60.47±1.00[c]	65.58±0.45[b]
T_p (°C)	85.39±0.64[a]	65.88±0.78[c]	69.43±0.15[b]
T_c (°C)	91.70±1.12[a]	79.32±0.84[b]	75.48±0.38[c]
ΔT (T_c-T_o)	10.59±0.65[b]	18.85±1.85[a]	9.90±0.09[b]
ΔH (J/g)	19.61±0.76[a]	19.67±0.41[a]	15.86±0.32[b]
PT (°C)	82.0±0.2[a]	66.9±0.3[c]	71.5±0.2[b]
PV (mPa·s)	844.0±5.1[b]	963.2±4.3[a]	743.9±3.3[c]
BDV (mPa·s)	109.5±2.4[c]	473.2±1.5[a]	288.4±1.8[b]
FV (mPa·s)	1354.0±7.4[a]	1044.0±6.3[b]	827.9±5.2[c]
SBV (mPa·s)	548.9±3.5[a]	514.4±4.1[b]	349.1±3.8[c]

671   T_o, T_p and T_c correspond to onset, peak and conclusion gelatinization temperature (°C); whereas ΔH and ΔT represent

672   melting enthalpy (J/g of starch) and gelatinization temperature range (°C) respectively. PT represents peak temperature

673   (°C), whereas PV, BDV, FV, SBV correspond to peak viscosity, breakdown viscosity, final viscosity and setback

674   viscosity (mPa·s) respectively.

675   Values in the table are means of three determinations (± standard deviation); values followed by the different letters

676   within a column differ significantly ($p < 0.05$).

677

678

679   Figures
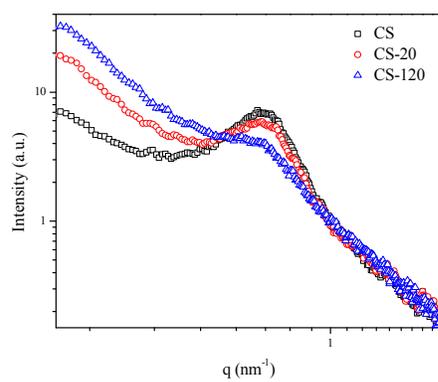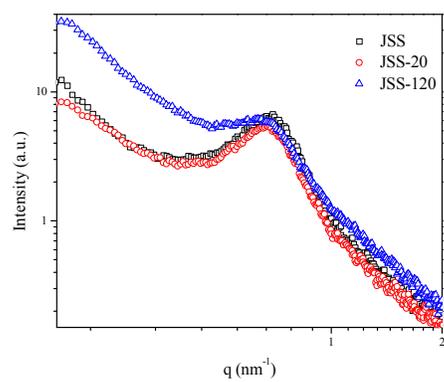
680

681

682   Fig 1

683
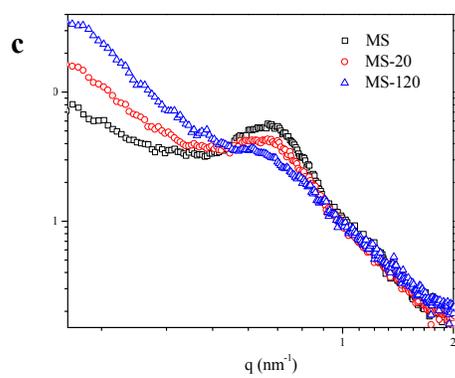
684

685   Fig 2

686

687

688   fig 3

689

690

691

692

693

694

695

696

697

698

699

700 Fig 4

701

a

c
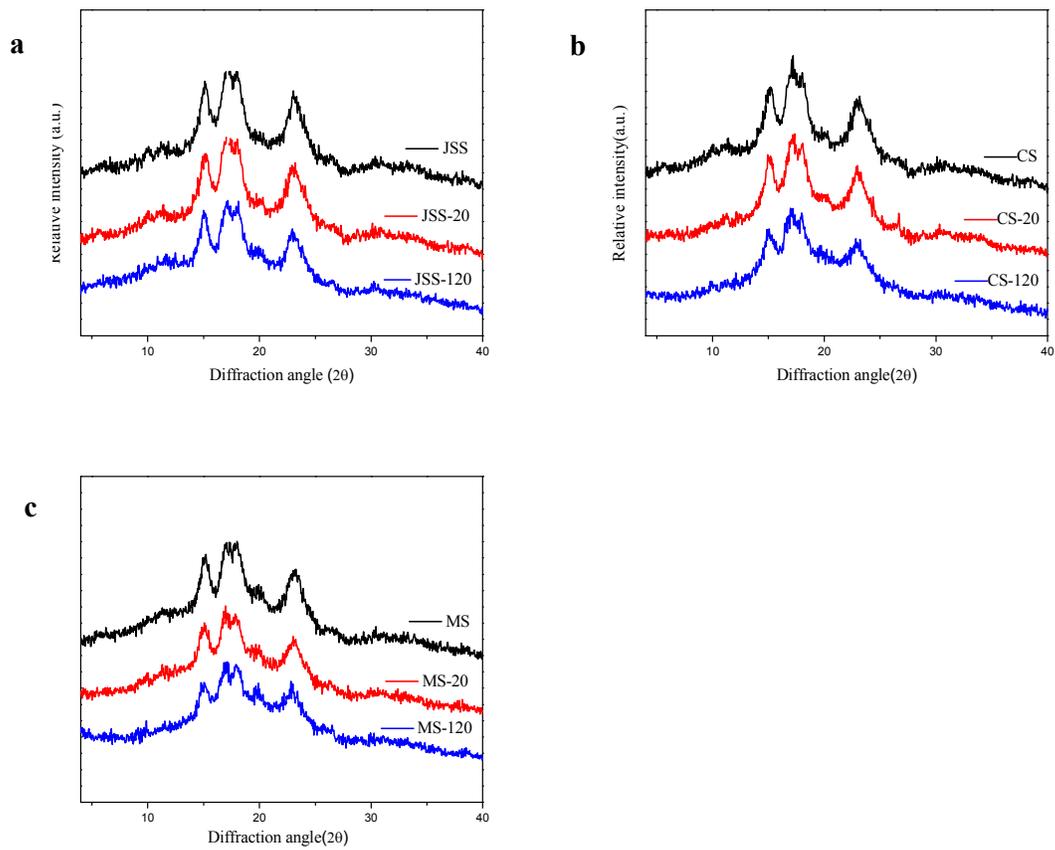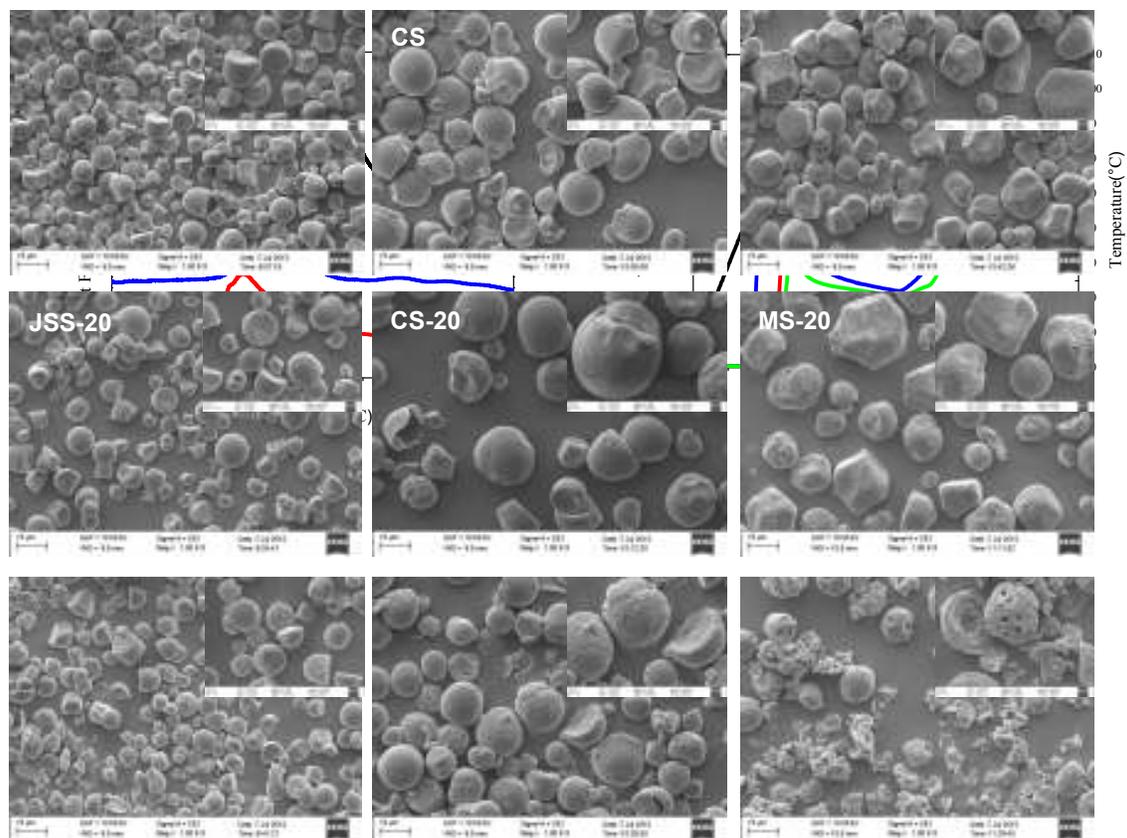

702

703

704

705

706

707

708

709

710

711   Fig 5

712

713

714

715

716

717

718

719

720